

# Investigation of two-stage electrostatic precipitation for silver removal from a helium stream

H.J. Steyn<sup>a</sup> R.T. Dobson<sup>a</sup>

<sup>a</sup>*Department of Mechanical and Mechatronic Engineering, University of Stellenbosch, Stellenbosch, South Africa*

---

## Abstract

In high temperature gas cooled nuclear reactors various unwanted particles have been found to plate out onto the surfaces of the primary circuit components. A simple deterministic deflection model is outlined in this paper to describe the deflection of charged silver nanoparticle particles in helium using the principle of electrostatic precipitation. An apparatus, consisting of a charging region and collection region, as in the case of two-stage electrostatic precipitators, was built to validate the applicability of the model. Notwithstanding its simplicity, it showed that it is able to favourably capture the experimentally determined particle deflection trajectories.

*Key words:* Electrostatic precipitation, two-stage, helium, silver, diffusion charging

---

## 1. Introduction

Electrostatic precipitators (ESP) have been widely used to remove suspended particles from a flowing stream of gas by means of an electrostatic force, such as in cement kilns, utility boilers, etc. [1]. An important advantage of ESPs is that the pressure drop is normally  $< 1000$  Pa [1], which reduces the pumping force needed to obtain the correct flow speed of the gas.

In ESPs a high voltage is applied to electrodes with different curvatures, which produces a corona discharge. The produced ions from this corona discharge then attach themselves to passing dust particles by means of field and diffusion charging, whereafter the particles migrate towards the collection electrode and subsequently plate-out on the surface of the collection electrode. When charged particles come into contact with the collection electrode, they are held to the plate by van der Waals and electrical attraction forces [2]. After contact the charge leaks to ground and the particles are only held to the plate by van der Waals forces. These collected particles can easily be removed by a process called rapping, where the collection electrode(s) are hit by a hammer and the particles then fall into a hopper. The advantages of rapping and low pressure drops provides

ESPs as a means for removal of unwanted particles in high temperature gas cooled nuclear reactors.

In high temperature gas cooled nuclear reactors various unwanted particles have been found to have plated out onto the primary circuit components of the reactor [3]. Personnel access for maintenance is limited as a result of some of these unwanted plated particles being radio-active [4]. This paper investigates a two-stage ESP as a candidate mechanism for removing silver particles from a helium stream. The reason for the use of two stages is attributed to the advantage of low particulate concentrations [2] and the ability to use an atmospheric pressure electrical discharge (APED) to create and charge the particles. Helium is an electronegative gas which carries little current up to its breakdown [2] and the current density influences the charge gained in the ionization zone of an ESP [1]. Therefore using an APED instead of a corona was investigated as a charging mechanism.

A simple deterministic deflection model is outlined in this paper to describe the deflection of charged particles. Due to its simplicity the model can then easily be used to make engineering design calculations for proposed ESPs. The deterministic deflection model's results are then compared to experimental results and conclusions are drawn. Recommendations as to the suitability of the proposed model to the described silver extraction process are also given.

---

*Email addresses:* [hs@hermanus.com](mailto:hs@hermanus.com) (H.J. Steyn), [rtd@sun.ac.za](mailto:rtd@sun.ac.za) (R.T. Dobson).

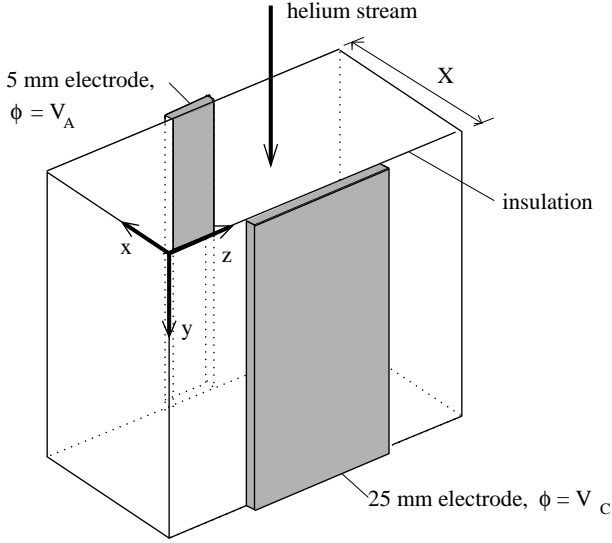


Fig. 1. The coordinate system

## 2. Deterministic deflection model

Figure 1 displays the coordinate system used. The direction in which the helium stream flows is  $y$ , the 25 mm electrode and 5 mm electrode are oriented along the  $z$ -axis and the distance between the two electrodes is given by  $X$ . The total applied force  $\mathbf{F}_{app}$  acting on a silver particle is given by

$$\mathbf{F}_{app} = \mathbf{F}_g + \mathbf{F}_{ES} + \mathbf{F}_D \quad (1)$$

where  $\mathbf{F}_g$  is the gravitational force, which can be expressed as

$$\mathbf{F}_g = m_{Ag}g \quad (2)$$

where  $m_{Ag}$  is the mass of the silver particle and  $g$  is the gravitational acceleration constant.

The coulombic force can be expressed as [5]

$$\mathbf{F}_{ES} = q\mathbf{E} \quad (3)$$

where  $q$  is the charge of the particle and  $\mathbf{E}$  is the electric field. The charge on the particle can be calculated by means of the saturation charge due to diffusion charging, as particles smaller than 100 nm are primarily charged by diffusion charging, while particles larger than 1  $\mu\text{m}$  are mainly charged by field charging [6]. In the intermediate size range of the particles a combination of field and diffusion charging of the particles occurs.

In diffusion charging the thermal energy of the ions is large, which implies that Brownian motion is also large. With this increased Brownian motion the velocity is large enough to overcome the Coulomb repulsive force between the particle and ion and further charging of the particle occurs [5] until

$$q_{dif} = 6\pi\epsilon_0 R \frac{k_B T}{e} \quad (4)$$

where  $k_B$  is Boltzmann's constant,  $T$  is the absolute temperature and  $e$  is the electron charge and  $R$  is the radius of the particle.

In the case of the Reynolds number ( $Re = \rho v_b D_h / \mu$  where  $\rho$  is the density of the helium,  $v_b$  is the bulk velocity of the helium,  $D_h$  is the hydraulic diameter and  $\mu$  is the viscosity of the helium) of the particle being less than 0.5, Stokes' law for the drag force on a sphere is applicable [7]

$$\mathbf{F}_D = -\frac{6\pi\mu R \mathbf{v}_{rel}}{C_m} \quad (5)$$

where  $\mu$  is the dynamic viscosity and  $\mathbf{v}_{rel}$  is the particle's velocity relative to the helium's velocity. When the Knudsen number  $Kn = \lambda/2R$  (where  $\lambda$  is the mean free path) tends to zero, the helium in which the particle is immersed is no longer continuous and must be treated as consisting of discrete particles. Due to this phenomenon Stokes' law needs to be corrected by the Cunningham corrections factor [2]

$$C_m = 1 + 1.246 \frac{\lambda}{R} + 0.42 \frac{\lambda}{R} \exp\left(\frac{-0.87R}{\lambda}\right) \quad (6)$$

The mean free path can be calculated as [8]

$$\lambda = \frac{1}{\sqrt{2}\sigma n} \quad (7)$$

where  $\sigma$  is the collision cross section, which is expressed as  $4\pi a^2$  with  $a$  being the radius of a helium atom. The number of molecules per unit volume  $n$  can be expressed as  $P/k_B T$  where  $P$  is the pressure of the helium.

To be able to calculate the electrostatic force  $\mathbf{F}_{ES}$  in equation 3 the electric field in the space between the two electrodes must be calculated. A  $x$ - $z$  plane (see figure 1) of the experiment is discretized into a grid of rectangular control volume elements. The electric potential  $\phi$  of each element was determined by applying the Laplace equation [9]

$$\nabla^2 \phi = 0 \quad (8)$$

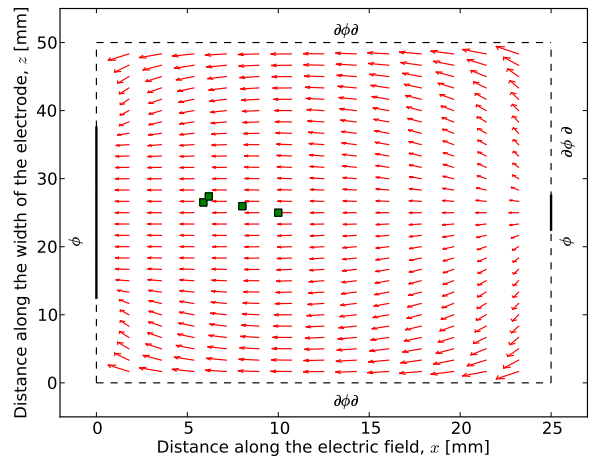


Fig. 2. The starting position of the particles inside the electric field

The electric potentials  $V_A$  and  $V_C$ , see figures 1 and 2, leads to a Dirichlet boundary conditions which have to be applied. For the other boundaries, which were insulated,

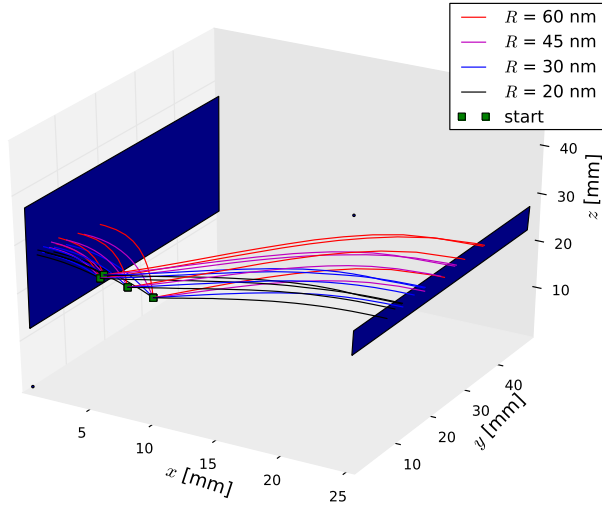


Fig. 3. Flight path of differently sized particles

the Neumann boundary values are used,  $\frac{\partial\phi}{\partial x} = 0$  or  $\frac{\partial\phi}{\partial z} = 0$ . Equation 8 is solved by applying these boundary conditions. The solution was then numerically differentiated to obtain the electric field, which is shown in figure 2.

When the particle reaches terminal velocity it no longer accelerates because the drag force is the same as the total applied force. Very small particles reach terminal velocity quite quickly. Kang [9] stated that if the characteristic time scale  $m_{Ag}/6\pi\mu R$  is an order of magnitude smaller than the time scale of the experimental observation, the above assumption is valid. Hence, the velocity of the particle moving at terminal velocity can be calculated by means of [9]

$$\mathbf{v} = \mathbf{v}_{he} + \frac{\mathbf{F}_{app}C_m}{6\pi\mu R} \quad (9)$$

The velocity of the helium  $\mathbf{v}_{He}$  is a function of  $x$  as the assumption was made that a laminar helium stream flows between two infinitely long plates and can be calculated by means of [10]

$$\mathbf{v}_{He}(x) = \mathbf{v}_b \frac{3}{2} \left( \frac{2x}{x_m} - \frac{x^2}{x_m^2} \right) \quad (10)$$

where  $x_m$  is the distance to the center of the channel.

The new position of a particle at time  $t + 1$ ,  $\mathbf{p}(t + 1)$  can be explicitly calculated knowing the old time  $t$  by

$$\mathbf{p}(t) = \mathbf{p}(t - 1) + \int_{t-1}^t \mathbf{v} dt + \Delta\mathbf{d}_{Br} \quad (11)$$

where  $\Delta\mathbf{d}_{Br}$  is the Brownian motion root-mean-square displacement, which can be expressed as [8]

$$\Delta\mathbf{d}_{Br} = \xi \sqrt{\frac{K_B T \Delta t}{3\pi\mu R}} \quad (12)$$

where  $\Delta t$  is the time step size. The random Gaussian vector  $\xi$  enables the Brownian motion term to vary in size and direction.

The silver particles were given random initial positions in the  $x$ - $z$  plane at  $y = 0$ , as shown in figure 2. The random

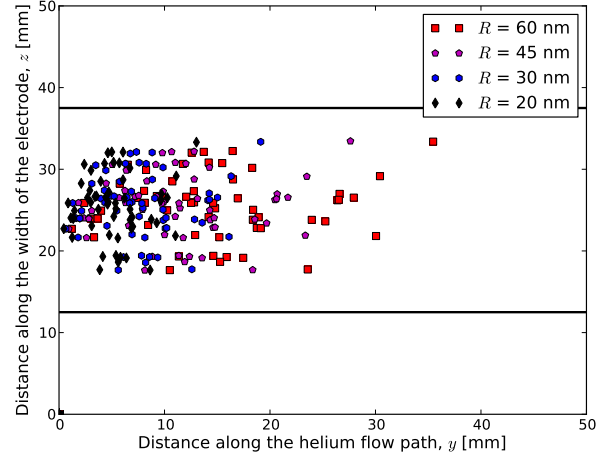


Fig. 4. Particle collection points on the 25 mm electrode surface

starting positions were generated using a normal distribution with  $\bar{x} = 8$  mm,  $\sigma = 1.25$  mm and  $\bar{z} = 12.5$ ,  $\sigma = 2.5$  mm. These values were chosen as they correspond with the experimental starting positions of the particles. The trajectories of 32 particles given in figure 3. There are four starting positions with four differently sized particles being charged positively and negatively. The positively charged particles are attracted towards the 25 mm electrode while the negatively charged particles are attracted towards the 5 mm electrode.

Figure 4 displays the positions of silver particles when they come into contact with the surface of the 25 mm electrode. From this figure it is clear that the most of the particles collect onto the 25 mm electrode before  $y$  of 30 mm.

### 3. Experimental work

Nanoparticles and microparticles were created by means of the gas aggregation technique, similar to the method employed by Mahoney and Andres[11]. They used an arc to evaporate atoms from a metal, whereafter the atoms were cooled by collisions with gas atoms, which induced homogeneous nucleation and nanoparticle formation. The schematic of the apparatus used in this study is shown in figure 5. Helium enters by two inlets creating two streams, namely primary and secondary. The secondary stream passes over an arc forcing the silver generated by means of the arc discharge to pass through the collimating glass sleeve into the helium flight path in the electric field. The arc is considered as the *first stage* of the ESP, the charging region, while the region between the two deflection electrodes is considered as the *second stage*, the collection region.

The voltage supply for breakdown was manufactured with the use of a flyback converter. By replacing the output resistor of the flyback converter with two silver electrodes spaced 0.5 mm apart, the energy is stored in the output capacitor until the breakdown voltage of the helium is

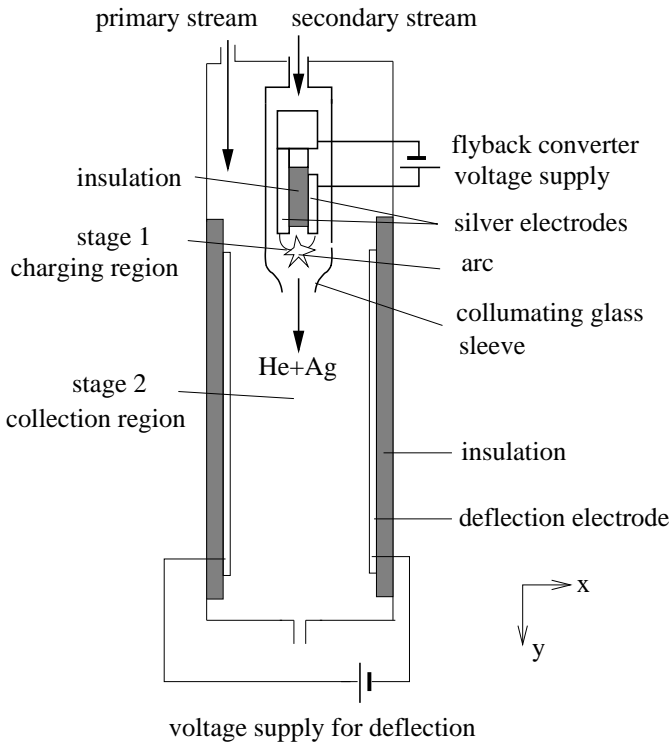
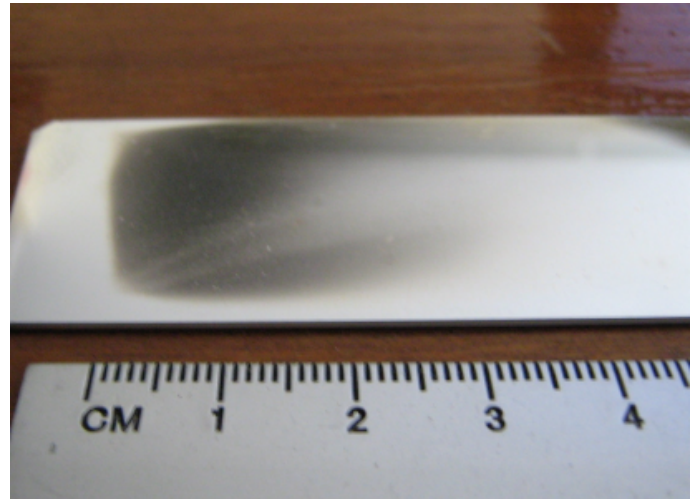


Fig. 5. The schematic of the experimental setup

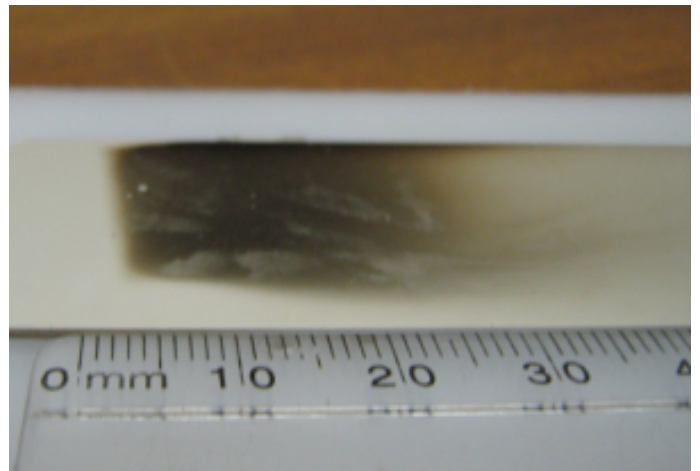
reached. A short arc pulse is created which reduces the energy in the capacitor. After the arc is extinguished the voltage increases again. This process is repeated and creates an ac atmospheric pressure electrical discharge (APED). According to Borra[6] an ac APED produces a bipolar charge distribution. This was experienced as silver collected on both of the deflection electrodes. The 25 mm deflection electrode was investigated as the surface roughness is less than  $20 \mu\text{m}$ , which was needed for use in an atomic force microscope (AFM).

Figures 6(a) and 6(b) display the 25 mm deflection electrodes of two separate tests which were done for a time duration of two hours. From these two figures it is clear that most of the particles collected before  $y$  of 30 mm, which is the same as which was predicted in the theoretical model in section 2. Note that the major difference between the two images is that the silver plating in figure 6(b) has a yellow tint, which is due to the the oxidation of the discharge electrodes after running the first test. Silver(I)oxide is gray, while silver(II)oxide is brown/black and silver(II)carbonate is yellow.

One of the deflection electrodes, which was an aluminium deposited glass slide, is displayed in figure 7. The flat surface in figure 7(a) is the aluminium covering on the glass slide, while the elevated areas are the deposited silver particles, which produces the colour in figure 6. The particle sizes as used in the calculations in section 2 were obtained from the cross-sectional profiles, such as displayed in figure 7(b). In this figure the left peak is a particle with a height of 40 nm and width of 750 nm.



(a)  $v_b$  of 0.0162 m/s.



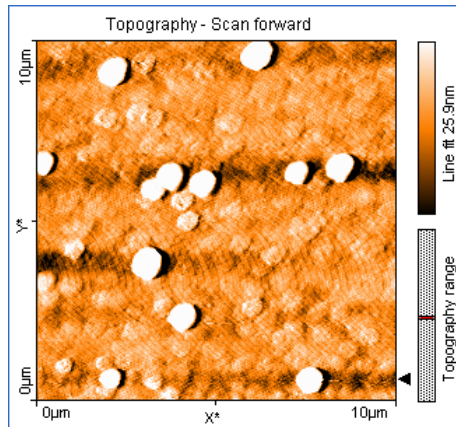
(b)  $v_b$  of 0.0169 m/s

Fig. 6. The 25 mm electrode with silver collected after tests with an electric field of 500 V over the 25 mm gap.

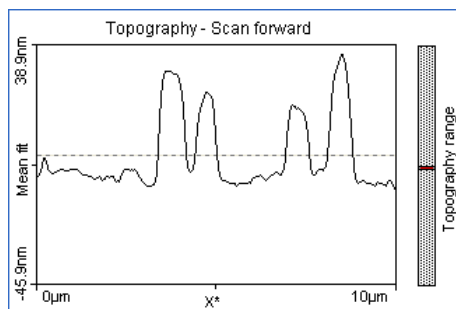
#### 4. Discussion and Conclusions

The experimental silver collection results shown in figure 6 compares favourably with the theoretical derived results given in figure 4. These favourable results validates the simple engineering model proposed in this paper for the use in designing a two-stage ESP for use in high temperature gas cooled nuclear reactors.

Notwithstanding the good correlation a number of assumptions were made. These are; the particles are charged up to their saturation charge limit, the velocity profile is fully developed laminar immediately after an obstruction (glass sleeve) is in the flow path, the empirically formulated Cunningham corrections factor is valid for helium and that re-entrainment does not occur. The assumption that re-entrainment does not occur, does not influence any of the results as the particles cannot re-enter the ionization zone before collecting further down the flight path. The Cunningham corrections factor has a large influence on the deflection of very small particles in particular. Equation 6 is



(a) Shaded view



(b) Cross sectional profile

Fig. 7. An AFM image of figure 6(a)

empirically formulated for particles suspended in air. As helium's mean free path is larger than that of air, the influence of Cunningham has been adapted accordingly by equation 7.

It is clear from the theoretical results, especially from figure 3, that the starting position of the particle has a large impact on its final resting position. Having an apparatus with a means of producing silver particles at a specific point more accurately is advised for future work. It is also advised to test higher helium velocities, higher pressures and temperatures.

## References

- [1] A. Mizuno, Electrostatic precipitation, *IEEE Trans. Dielectr. Electr. Insul.* 7 (5) (2000) 615–624.
- [2] K. Parker, *Electrical operation of electrostatic precipitators*, Institute of Electrical Engineers, London, 2003.
- [3] R. Bäumer, *AVR- experimental high-temperature reactor*, VDI Verlag, Düsseldorf, 1990.
- [4] J. van der Merwe, Development and application of the PBMR fission product release calculation model, *Nucl. Eng. Des.* 238 (2008) 3092–3101.
- [5] D. Taylor, P. Secker, *Industrial Electrostatics: Fundamentals and Measurements*, Wiley, Taunton, 1994.
- [6] J. Borra, Charging of aerosol and nucleation in atmospheric pressure electrical discharges, *Plasma Phys. Contol. Fusion* 50 (124036).

- [7] C. Crowe, D. Elger, J. Roberson, *Engineering Fluid Mechanics*, 7th Edition, Wiley, New Jersey, 2001.
- [8] F. Sears, *An Introduction to Thermodynamics, the Kinetic Theory of Gasses, and Statistical Mechanics*, 2nd Edition, Addison-Wesley, 1964.
- [9] K. Kang, X. Xuan, Y. Kang, D. Li, Effects of dc-dielectrophoretic force on particle trajectories in microchannels, *J. Appl. Phys.* 99 (064702).
- [10] W. Rohsenow, H. Choi, *Heat, mass and momentum transfer*, Prentice Hall, New Jersey, 1961.
- [11] W. Mahoney, R. Andres, Aerosol synthesis of nanoscale clusters using atmospheric arc evaporation, *Mater. Sci. Eng.* 8 (1995) 160–164.